JOURNAL OF MATERIALS SCIENCE 12 (1977) 1499–1518

Review
HTGR fuel rods: carbon-carbon composites designed for high weight and low strength

R.E. BULLOCK
General Atomic Company, San Diego, California, USA

The evolution of the process for fabricating fuel rods for the high-temperature gas-cooled reactor (HTGR) by injection and carbonization of a thermoplastic matrix that bonds close-packed beds of pyrocarbon-coated fuel particles together is reviewed for the fresh-fuel cycle, and a variant process involving a thermosetting matrix that would allow free-standing carbonization of refabricated fuel is discussed. Previous attempts to fabricate such injection-bonded fuel rods from undiluted thermosetting binders filled with powdered graphite were unsuccessful, because of damage to coatings on fuel particles that resulted from strong particle-to-matrix bonding in conjunction with large matrix shrinkage on carbonization and subsequent irradiation. These problems have now been overcome through the use of a diluted thermosetting matrix with a low-char-yield additive (fugitive), which produces a more porous char similar to that from the pitch-based thermoplastic used in fabrication of fresh fuel. A 1-to-1 dilution of resin with fugitive produced the optimum binder for injection and carbonization, where the fired matrix in such rods contained about 20 wt % binder char and 80 wt % powdered graphite. Thermosetting fuel rods diluted with various amounts of fugitive to give binder chars that range from 12 to 48 wt % of the fired matrix have been subjected to irradiation screening tests, and rods with no more than 32 wt % binder char appear to perform about as well under irradiation as do pitch-based rods. However, particle damage does begin to occur in those lightly diluted rods in which the less-stable binder char constitutes more than 32 wt % of the fired matrix. Finally, while the finished products are quite different, it is pointed out that aims in the fabrication of fuel rods and in the initial carbonization step to convert fibrous-reinforced plastics into structural carbon–carbon composites are similar and that more exchange of ideas and techniques in these areas might be beneficial.

1. Introduction

The purpose of this paper is to call attention to an important type of carbon–carbon composite designed for high-temperature functions which are quite different from those of high-performance structural composites. The composites in question are fuel rods for the high-temperature gas-cooled reactor (HTGR), which is designed to convert nuclear heat into electrical energy [1–5]. These cylindrical fuel rods consist of close-packed carbon-coated spheres of nuclear materials (fuel particles) and of high-conductivity graphite granules (shim particles) that are bonded together with a carbonaceous matrix filled with graphite flour. These rods are inserted into blind fuel holes drilled into hexagonal graphite fuel blocks, which stack on one another to form the core of the HTGR, and the heat generated in these closed fuel channels during reactor operation is conducted away by helium gas that flows through adjacent inter-

spersed coolant holes that are aligned from block to block. The primary function of the gas-tight pyrocarbon coatings on fuel particles is for the retention of fission products, while the fuel rod matrix is intended to bind together and protect fuel particles from mechanical damage and/or spillage that might occur if loose particles were thermal cycled in fuel blocks, to increase the thermal conductivity beyond that for unbonded particle beds, and to provide secondary containment for any fission products that escape from defective fuel particles. A third level of containment is provided by the graphite partition separating fuel and coolant channels in fuel blocks.

The heart of the fission-product containment system in the HTGR is the coated fuel particle; this sand-grain-sized particle, which is coated in a high-temperature fluidized bed by chemical vapour deposition, is an interesting structural composite in itself. In the present fresh-fuel design for the HTGR, there are two types of coated particles: fissile particles, which provide the initial power source in a new reactor core, and fertile particles, in which fissionable material is bred during reactor operation. Fissile particles contain 200 μm spherical kernels of UC_2 (having a U^{235}/U ratio of 93%) that are consecutively coated with four distinct layers: (1) porous pyrocarbon (PyC), (2) inner dense PyC, (3) SiC, and (4) outer dense PyC. The porous 100 μm buffer layer provides void space for accommodating any pressure buildup from gaseous fission products, the 25 μm inner PyC holds up most fission products and thereby protects the neighbouring SiC from chemical attack, the 25 μm SiC layer provides enhanced resistance to the migration of certain metallic fission products and carries much of the stress imposed by irradiation effects (because of its high elastic modulus), and the 35 μm outer PyC protects the SiC reinforcement from chemical and mechanical damage. Fertile particles, which undergo much lower percentages of fissions during their reactor lifetimes, consist of 500 μm spherical kernels of ThO_2 that are coated with only two layers of PyC: a porous 85 μm buffer layer, and a 75 μm dense layer. Thus, overall diameters of fissile and fertile design particles are 570 and 820 μm respectively, with 4.3 and 22.7 vol% of each particle being devoted to nuclear fuel.

In addition to the operational benefits cited above, coated fuel particles also provide handling advantages during fuel fabrication, and the non-burnable SiC layer on fissile particles allows for easy separation of this high-burnup kernel material during fuel reprocessing. All aspects of the coated particles themselves have been well documented in the literature, including several comprehensive review articles [6–11]. However, very little information has been published on fabrication of fuel rods with close-packed particle inclusions of this type, which is the subject of this paper. The fabrication techniques to be summarized have evolved in the USA over a period of years and reflect the combined efforts of a number of investigators at General Atomic Company (GAC) and at Oak Ridge National Laboratory (ORNL). European work on fuel bodies for gas-cooled reactors has developed along different lines, for the most part, and will receive only brief mention. Before proceeding to fabrication details, a brief survey will be given as to why HTGR fuel rods have been designed for high weight and low strength. It is desirable to obtain the highest uniform power density possible in the core, to minimize the size of the prestressed concrete reactor vessel (PCRV) that provides for large-scale containment of fission products, and this requires maximizing the heavy metal weight in fuel rods that are located near the outer circumference of the cylindrical core. In order to do this, a fuel-rod fabrication process was developed in which a low-viscosity matrix was injected into a random close-packed bed of well mixed fissile and fertile fuel particles. Then, in order to hold the size of the fuel rod constant, graphite shim particles were added to rods in the central portion of the core where less nuclear fuel was required. Unlike fibrous-reinforced structural composites, where the aim is to force the stronger fibre inclusions to fail before the weaker matrix does, a fuel rod is designed in such a way that the matrix and/or its interface with particles must always fail at stress levels that are low enough to prevent damage to the coated particle inclusions.

2. The present fabrication process and its evolution

The present process for fabricating HTGR fuel rods is briefly summarized as follows: (1) fissile, fertile, and impregnated graphite shim particles, sufficient to fill a 15.7 mm cylindrical mould to a height of approximately 64 mm, are blended and poured into a heated mould, (2) a molten pitch-

based matrix filled with graphite flour is injected into this random close-packed particle bed (containing about 60 vol% particles) at pressures low enough to prevent damage to coatings on fuel particles, and (3) after cooling the solidified fuel rod is ejected from the mould. Finally, (4) 1584 of these "green" rods are loaded into 15.85 mm blind fuel holes (12 rods in each of 132 holes) in a hexagonal graphite fuel block that is 79 cm high and 36 cm across the flat lateral surface; these rods are heat-treated in the block to temperatures in excess of 1500° C (in an inert atmosphere) to drive off volatiles from the pitch-based binder, leaving the particles weakly bonded together by the resulting porous carbon char. The fueled region of a 1160 MW(e) HTGR core will contain about 4000 such fuel blocks [5], totalling some 6 million fuel rods. Moreover, the average fuel rod in such a core will contain roughly 22 000 fuel particles; about 9000 of the smaller fissile particles (7 vol%) and 13 000 of the larger fertile particles (30 vol%). Thus, there are roughly 10^{11} active fuel particles in such a core, not including half this number of graphite granules (700 to 900 μm diameter) that are used to shim out rod lengths and to increase their thermal conductivities. The evolution of this fabrication process will be developed by examining the three generations of HTGRs designed by GAC.

2.1. Peach Bottom Reactor

The prototype HTGR designed by GAC was the 40 MW(e) Peach Bottom reactor [12], which began producing electricity in early 1967 [13]. This reactor used an annular fuel compact of the same general type as those developed in the UK for the Dragon reactor [14]. These fuel bodies contained only about 25 vol% particles; they were fabricated by admix compaction and subsequent heat treatment of a carbonaceous matrix that contained dispersed fuel particles. This early work (to mid-1967) on lightly loaded fuel bodies in the USA and in Europe has been well summarized by Goeddel [13], and the subsequent evolution of European fuel bodies has also been well documented: the annular Dragon compacts in the UK [14–19], pebble-bed fuel in West Germany [20–23], and CERCA rods in France [24, 25]. However, fuel-body work for gas-cooled reactors in the USA, which began to diverge from that in Europe after mid-1967, has not been as well reported; this will be the starting point of the present paper, and some interesting differences in design objectives and similarities in process techniques between HTGR fuel rods and structural carbon–carbon composites will be pointed out along the way.

2.2. Fort Saint Vrain Reactor

The hexagonal graphite fuel block with separate fuel and coolant channels was adopted for the larger 330 MW(e) Fort Saint Vrain (FSV) demonstration plant [1, 2]. Initially, fuel channels were to be filled with loose coated particles whose interstices were infiltrated with powdered coke for increased fission-product adsorption [2, 13]. However thermal-cycling tests soon revealed that such loose particle beds tended to settle as particles filled the radial gaps that developed during heat up because of the greater thermal expansion of the graphite fuel block. Then, during cooldown, fuel particles were squeezed by the graphite block as it attempted to return to its initial dimensions; this thermal-ratcheting effect dictated that fuel particles be bonded together to form rods. The usual two-step fabrication process for bonded fuel bodies that operate at high temperatures is as follows: first, in the consolidation step, particles contained in a mould are bonded together under pressure with a putty-like matrix, which consists of a liquid organic binder filled with graphite flour. Through temperature variations, this matrix is quickly hardened around the particle inclusions, and the unfired "green" fuel body is removed from the mould. Then, in a second carbonization step, the fuel body is heat-treated to drive off volatiles from the binder, leaving the fuel particles bonded together with a carbon char that is filled with powdered graphite. This same general procedure was followed in fabricating rods to go in the graphite fuel blocks, but quite different fabrication techniques from those developed in Europe [14–25] were eventually adopted for both process steps. Previously the fabrication process used for the consolidation step was a variation of admix compaction in which fuel particles were first mixed with matrix constituents and all components were then pressed together. To obtain maximum heavy metal loading (uranium plus thorium), an injection-moulding process (ideal for mass pro-

duction) was adopted in the USA in which the matrix was intruded into random beds of close-packed fuel particles contained in metal moulds.

2.2.1. Injection-moulding process

The two process steps that are unique to injection-moulding of fuel rods involve random particle packing in the mould, and intrusion of the matrix through the network of interstices between close-packed spheres along the entire length of the particle bed.

2.2.1.1. Random close packing of particles. It is instructive to examine the various regular arrangements of spherical particles before considering the case of random packing, and in doing this it will be convenient to begin with the simpler case for regular packing of cylindrical inclusions in an idealized unidirectional composite slab [26]. The maximum volume packing fraction ν in such a slab filled (n to the row) with long collimated cylinders of the same diameter d that are stacked directly on one another (m to the column) to form a rectangular array in which each interior cylinder touches four of its neighbours is given by $\pi/4 = 0.785$; this increases to $\pi\sqrt{3}/6 = 0.907$ when cylinders in every other one of the large number of rows are displaced by one-half diameter in the width direction, allowing the stack height to drop from md to $md\sqrt{3}/2$ as each cylinder settles into the space between cylinders below to form a hexagonal array in which each interior member touches six of its neighbours. Two thirds of the original volume remains when a long cylinder is cut down into k spheres of the same diameter; therefore, from the simpler cylindrical case, ν for a slab filled with a cubic array of touching spheres is $\pi/4 \times 2/3 = 0.524$, while ν for spheres staggered in the width direction is $\pi\sqrt{3}/6 \times 2/3 = 0.605$. Each interior sphere touches 6 and 8 of its neighbours respectively, in these two arrangements, which are referred to as simple cubic and as single staggered or orthorhombic. The extra freedom of arrangement obtained by decoupling the cylindrical inclusions into spheres will produce larger contact numbers and higher values of ν for the remaining regular arrangements of touching spheres.

In particular, a second staggering of every other particle slice along the length of the slab by $d/2$ in the width direction shortens the overall length from kd to $kd\sqrt{3}/2$, which produces a ν of $\pi\sqrt{3}/9 \times 2\sqrt{3}/3 = 0.698$. This double-staggered or tetragonal-spheroidal arrangement has a contact number of 10. Finally, a displacement of each sphere in every other thickness layer by $d\sqrt{3}/6$ in the length direction allows spheres to settle into deeper void spaces between three spheres that touch to form triangles, which further shortens the stack height by a factor of $2\sqrt{2}/3$ (from $md\sqrt{3}/2$ to $md\sqrt{6}/3$), and ν for this dense-packed hexagonal arrangement in which every interior sphere touches 12 other spheres is given by $2\pi/9 \times 3\sqrt{2}/4 = 0.740$. Another arrangement with a contact number of 12 can be obtained by going back to the single-staggered case and displacing each sphere in every other thickness layer by $d/2$ in the length direction, which allows spheres to settle into still deeper void spaces between four spheres that touch in a square array. This face-centred cubic arrangement shortens the overall stack height by a factor of $\sqrt{6}/3$ (from $md\sqrt{3}/2$ to $md\sqrt{2}/2$), and this also gives $\nu = \pi\sqrt{3}/9 \times \sqrt{6}/2 = 0.740$. Both of these arrangements with contact numbers of 12, which give the maximum possible volume packing fraction for spheres of the same size, are usually lumped together and referred to as regular dense-packed or rhombohedral arrangements.

Thus, when the container is assumed to have dimensions that are large compared to the diameter of a single sphere, the various regular symmetrical arrangements of equal spheres give packing percentages that range from 52.4 to 74.0% of the space in which they are contained, no matter what its shape. However, the arrangements that give these two extreme packing percentages are unstable and do not occur in random packing experiments where spheres are simply poured into containers [27]; consequently, some combination of single and double staggering is to be expected. Experimental studies on random packing of equal spheres show the actual maximum packing fraction to be 0.636 ± 0.001 [28], which is exactly the value that would be obtained for a 2-to-1 weighting of the single- and double-staggered arrangements. Moreover, this value is independent of container shape and sphere size for a container whose smallest dimension (x_{min}) is large ($x_{min} > 20d$) compared to the diameter d of a sphere [27]: it might be oranges in a rectangular crate, gum balls in a spherical dispenser, or coated fuel particles in a cylindrical mould. The smallest experimental random packing fraction that can be obtained from a gentle filling of a container with equal spheres is about 0.60, which is roughly equal to

that for the single-staggered arrangement. However, a slight tapping of the container will cause this so-called loose random packing arrangement to shift and assume the dense random packing fraction of 0.636, which is the value appropriate for coated particles of one size in an injected fuel rod. The various regular and random arrangements that have been discussed for inclusions of one size are summarized and compared in Table I.

The packing fraction for fixed proportions of spheres of two different sizes increases steadily above that for equal-size spheres as size differences become more and more pronounced, and ν for any given diameter ratio reaches its maximum value for about 73 vol % large spheres and 27 vol % small spheres [34]. The reasoning here, of course, is that packing is maximized when the number and size of the smaller spheres are selected in such a way that they best fill the voids between the larger spheres. Binary packing fractions in excess of 0.80 are reached for optimum proportions of spheres that have diameter ratios of 10 or more, but little additional packing is gained when the diameter of the larger sphere is less than twice that of the smaller one [34]. The larger fertile particles in HTGR fuel rods are mixed with the smaller fissile particles in roughly a 4:1 ratio by volume, which is favorable for dense packing. However the diameter of the fertile particle is only 1.43 times as large as that for the fissile particle, and this produces a packing only slightly in excess of that for one particle type. Moreover, in the current design, the average fuel rod contains about 23 vol % of irregular graphite shim particles, which do not pack as efficiently as the spherical fuel particles [35]. Therefore, the packing fraction in the average fuel rod is equal to only about 0.60.

2.2.1.2. Intrusion of Matrix into Particle Beds At this point, a random bed of well-mixed fuel particles has been formed in which 60% of the mould volume is occupied by particles and 40% is vacant and available for injection with an organic binder, which must be reduced to a char during a subsequent carbonization step. Such a binder without particle inclusions undergoes a large volume shrinkage during carbonization (up to 50% for an unfilled binder), and this causes internal (and often, external) cracking in a fuel rod with touching particles, which prevent gross shrinkage of the binder. This internal shrinkage can be reduced (in rough accordance with the law of mixtures up to 50 vol % filler) by introducing a filler material into the binder that undergoes little or no shrinkage during carbonization, and finely powdered polycrystalline graphite is an excellent material for this purpose. Graphite flour does not shrink during carbonization, since it has already been heat treated to a higher temperature than that to which coated particles can be subjected, and the resulting graphite-filled binder has a higher thermal conductivity than that pertaining to the less crystalline binder char alone. The next problem to be addressed concerns the injectability of such a

TABLE I Packing fractions for various arrangements of touching inclusions

Inclusion type	Packing arrangement	Contact number	Volume packing fraction*
Cylinder	Rectangular	4	$\nu_1 = \pi/4 = 0.785$
	Hexagonal	6	$\nu_2 = \nu_1 \times 2\sqrt{3}/3 = 0.907$
Sphere	Simple cubic	6	$\nu_3 = \nu_1 \times 2/3 = 0.524$
	Single staggered	8	$\nu_4 = \nu_3 \times 2\sqrt{3}/3 = 0.605$
	Double staggered	10	$\nu_5 = \nu_4 \times 2\sqrt{3}/3 = 0.698$
	Dense-packed hexagonal	12	$\nu_6 = \nu_5 \times 3\sqrt{2}/4 = 0.740$
	Face-centered cubic	12	$\nu_7 = \nu_4 \times \sqrt{6}/2 = 0.740$
	Random loose packing	8†	$\nu_8 = 0.60 \approx \nu_4$
	Random dense packing	8.7†	$\nu_9 = 0.636 = 2\nu_4/3 + \nu_5/3$

*It is noteworthy that when the simplest solids consisting of frozen inert gases are allowed to melt, the reduction in density ($\rho_{\text{liquid}}/\rho_{\text{solid}} = 0.862$) agrees almost exactly with that predicted for a change from a regular to a random dense packing of spheres [29], where $\rho_{\text{random}}/\rho_{\text{regular}} = 0.860$. Also, the radial distribution of atoms in these liquids agrees very well with that found for random dense packing of spheres [30]. This modelling of the structure of liquids by random packing of spheres, first proposed by Bernal [31, 32], has stimulated a great deal of the work done on packing arrangements.

†Contact numbers for random packing were taken from [33]. Notice that these experimental contact numbers are consistent with the assumption that random loose packing is the single-staggered arrangement and that random dense packing is a 2-to-1 weighting of the single- and double-staggered arrangements.

particle-filled binder (hereafter called the matrix) through a random close-packed bed of larger fuel particles.

The two types of interstices for dense regular packings of spheres are the "triangular" voids between three spheres that touch to form a triangle and the "square" voids between four spheres that touch to form a square [36]. For coarse spheres of one size, the diameter of the largest fine sphere that will pass through each of these two types of interstices is given by $d_f = d_c\ (2\sqrt{3} - 3)/3 = 0.155 d_c$ and by $d_f = d_c\ (\sqrt{2} - 1) = 0.414 d_c$ for triangular and square voids, respectively [27]. Therefore, fine spheres will pass through any path of the continuous labyrinth formed by a random close-packed bed of coarse spheres that are at least 6.5 times as large in diameter as the fines [36]. The smallest void in a random bed of HTGR fuel particles is the triangular one between three 570 μm fissile particles, and a spherical filler particle with a diameter of less than 88 μm would pass through this opening. The largest particle in the graphite filler for the fuel rods has been set at less than one-half this size (40 μm), with 95% of the size distribution being less than 15 μm, so that these particles should readily pass through all possible paths within the fuel-particle bed for matrices with filler levels low enough to prevent bridging (or filtration).

The ideal fuel rod would be one in which the 40% space not occupied by fuel particles was subsequently filled with a second random close packing of spherical graphite filler particles, and the remaining 15% voidage between the fine filler component would then be injected with the liquid binder. For typical filler and binder densities of 2.2 and 1.2 g cm^{-3} respectively, this would entail a matrix with 75 wt% filler. The graphite flour is not spherical however, and the best random packing that can be realized at the compaction pressures in question is about 0.56; this reduces the ideal filler content of the matrix to 70 wt%. In practice, the matrix mixture must be injectable through the full length (64 mm) of a fuel rod in about 1 min for pressures that do not exceed 70 kg cm^{-2}, and experience has shown that such axial injection can be done only for filler contents of 40 wt% or less. Thus, the penalty paid for the gain in fuel loading in going from admix compaction to injection is that the filler content of the matrix must be reduced to about one-half of that used in European-type rods for gas-cooled reactors; this leads to increased matrix shrinkage during carbonization and irradiation, all of which must now occur internally by creation of microvoids in the matrix and/or by opening up of gaps between the matrix and particle inclusions. The accommodation of this increased internal shrinkage, without causing coating damage through particle–matrix interactions or rod damage through external cracking and deformation, constitutes a very severe requirement for injected matrix material. The severity of this shrinkage problem could be reduced if multi-channel lateral injections can be used to deliver higher filler contents over shorter path lengths, but radial injections of this type complicate rod removal from the moulds and are not yet fully perfected.

2.2.2. Carbonization and irradiation testing of rods

Once the two-step consolidation process described has been completed and hardened "green" rods have been removed from moulds, the critical carbonization step must then be performed to prepare the rods for high-temperature service in the reactor; this final fabrication step and the subsequent irradiation performance of the rods are the critical tests that must be used to optimize the matrix formulation of the previous consolidation step, which is not nearly so severe. The difference in process difficulty between the consolidation and carbonization steps is roughly equivalent to that involved in going from a carbon-fibre reinforced plastic to a structural carbon–carbon composite. Two general classes of matrices have been evaluated: (1) thermosetting, which can be heat-treated free standing without loss of shape, and (2) thermoplastic, which must be restrained during heat treatment. The carbonization and irradiation testing of each of these matrix types will be briefly described in the chronological order in which they occurred.

2.2.2.1. Thermosetting matrix. The first injection-bonded fuel rods to be fabricated and irradiation tested were thermosetting rods that used undiluted resins as binders, but these were not generally acceptable because breakage of the pyrocarbon coatings on fuel particles sometimes occurred during carbonization [37] and often occurred during irradiation [38, 39]. The causes for these damaging particle–matrix interactions were two-fold: the strong, high-char-yield thermosets remained tightly bonded to the fuel particles, and at the same time they underwent large internal

shrinkages during both heat treatment and subsequent irradiation, which tended to fracture the coatings and pull them away from the fuel kernels. The strong particle-to-matrix bonding in as-made rods of this type is illustrated in the polished cross-section of Fig. 1, and the coating damage produced in such an irradiated rod is shown in Fig. 2. More recent work (Section 3) has shown that the strength and bondability of thermosetting matrices can be reduced to acceptable levels by diluting resins with low-char-yield additives to produce microporosity therein, which also limits shrinkage, and that such modified rods perform well under irradiation. This was not known then, however, and work was suspended on thermosetting rods for several years because of the unfavorable early results produced by excessive shrinkage of undiluted binders that were too strong and too well bonded to particles.

2.2.2.2. Thermoplastic matrix. A pitch-based thermoplastic matrix, which was known to produce a weaker more-porous structure when carbonized, was tried next in the hot-injection moulding of rods, and both carbonization and irradiation performances of these rods improved dramatically [40, 41]. The much weaker particle-to-matrix bonding in the pitch-based rod is apparent from a comparison of Figs. 3 and 1, and the more-porous structure of the matrix char itself is illustrated in Fig. 4. The weak matrix needed to eliminate coating damage for the heavy fuel loadings of the injection process was now available, but the drawback in switching from a strong thermosetting matrix to a weaker thermoplastic one was that rods could no longer be carbonized free standing, for they now had to be closely contained during the stage when the matrix becomes molten in order to prevent loss of shape.

The method selected for providing this restraint during carbonization of rods for the FSV demonstration plant was the powdered-bed procedure [42] in which rods were vibratory-packed in fine alumina powder during the first phase of their carbonization [43]. During this initial phase, rods were uniformly heated to 800° C in an inert environment for 2 h, then cooled, removed from the powdered bed, and lightly brushed to remove surface alumina. In the second phase of carbonization, these free-standing rods were uniformly heated to 1800° C in an inert environment for 1 h, with a half hour hold at the maximum temperature. The heat-treatment cycle was separated into these two phases to prevent high-temperature reactions between the rods and the powdered alumina [43].

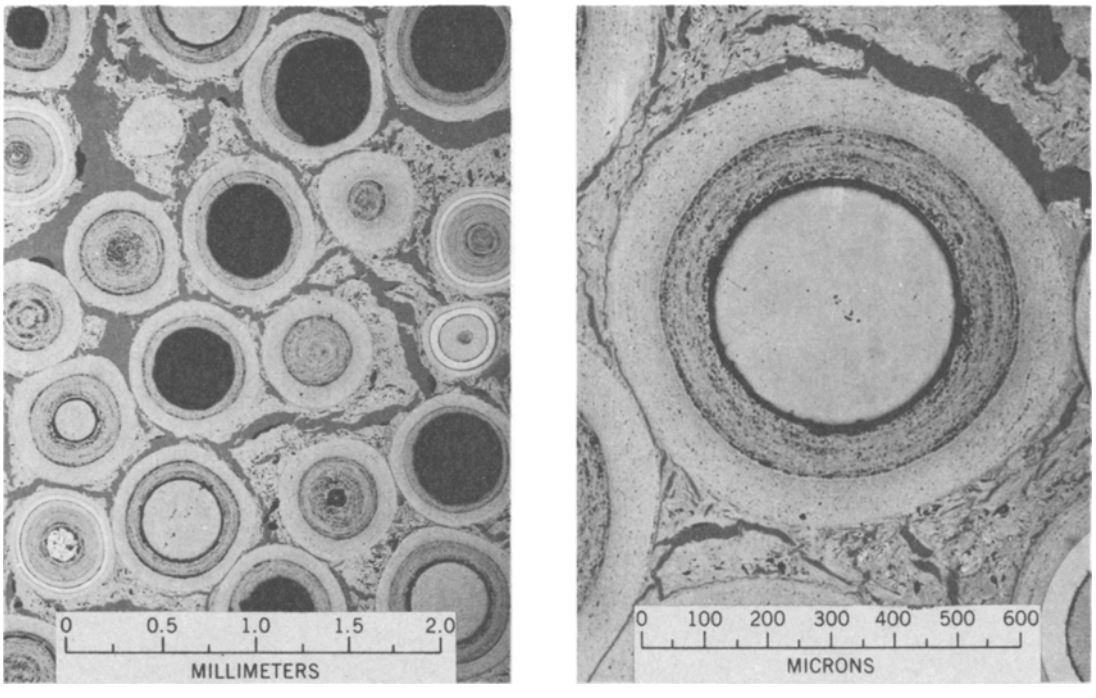

Figure 1 Strong particle-to-matrix bonding coupled with large internal shrinkage in an undiluted thermosetting rod.

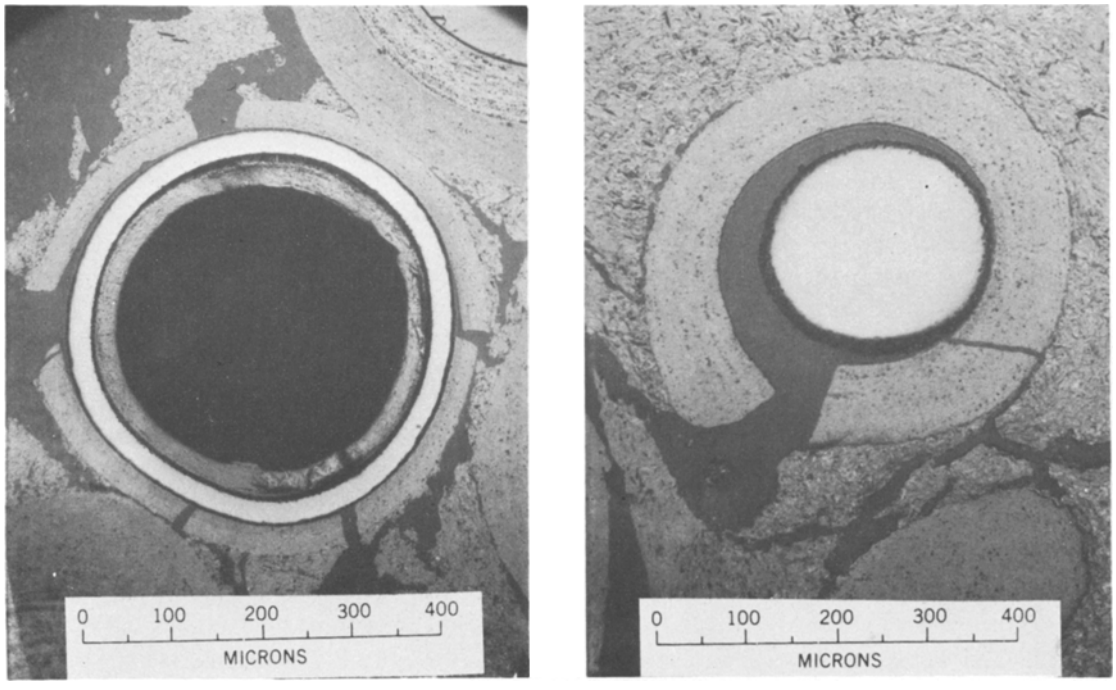

Figure 2 Coating damage in an irradiated rod having an undiluted thermosetting matrix.

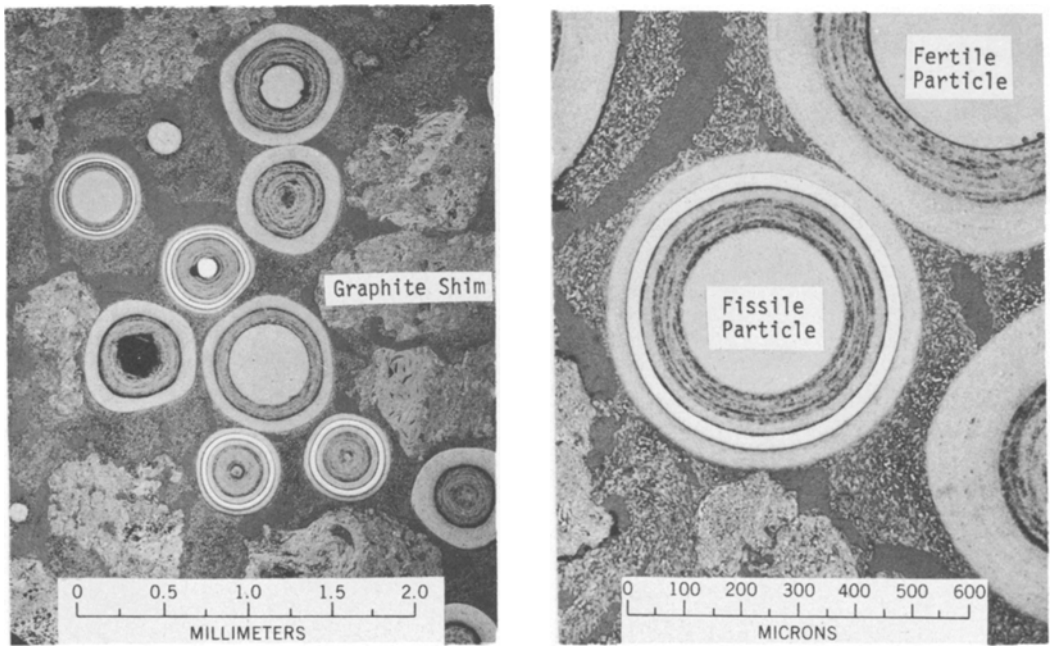

Figure 3 Matrix structure in a thermoplastic pitch-based rod.

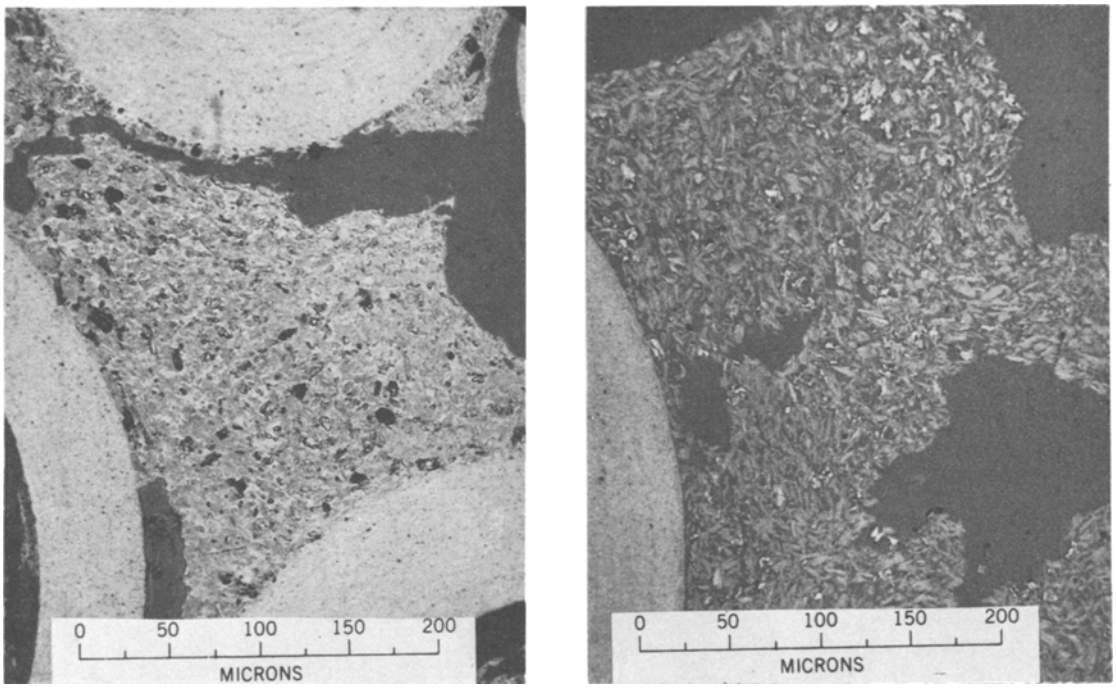

Figure 4 Comparison of porosity in matrices derived (a) from an undiluted resin and (b) from pitch.

2.2.2.3. Shrinkage problem common to both matrix types. In addition to the strong interaction problem, which was solved with the use of the weaker, less strongly bonding pitch-based matrix, there remains the problem of the matrix shrinkage itself. An undiluted organic matrix of any type that contains the maximum 40 wt % filler allowed by the current injection process undergoes bulk volume shrinkage in excess of 30% when heat-treated to 1800° C without particle inclusions, and the additional irradiation-induced shrinkage of such unrestrained matrix is on the order of 10% [38]. The touching particles in close-packed fuel rods prevent such gross shrinkages, of course, but then internal cracking of the matrix is almost certain to occur because of the buildup of restrained-shrinkage stresses [44–46]. This together with all of the finer-scale internal shrinkage that follows is sure to further weaken the matrix, but it is recalled that the only strength requirement of the matrix is to hold coated particles in place within undisturbed fuel rods during their lifetime in the reactor.

The objective, then, is to limit matrix damage to discontinuous types of hairline cracks that will not compromise rod integrity for the limited service requirement intended. This has also been accomplished more successfully with a pitch-based matrix than with an undiluted thermoset, which undergoes larger shrinkages and sustains larger stresses before cracking occurs. This same problem of shrinkage cracking is also encountered in the carbonization of organic binders reinforced with high volume fractions of carbon fibres [47, 48], and there too a pitch binder is found to perform better than a thermoset [49, 50]. Both types of unfilled binders crack rather badly however, and this necessitates multiple impregnations and *in situ* carbonizations of such binders to produce acceptable structural carbon–carbon composites [51, 52]. Consequently, chemical vapour deposition (CVD) of a type similar to that used in coating fuel particles is often employed [53, 54], and this avoids the problem of carbonization shrinkage altogether. The CVD process would probably also work well for bonding particles into fuel rods, but the process would be very difficult to scale up for production of the millions of fuel rods required for each reactor. Also, such a pyrocarbon deposition would probably be highly anisotropic and, therefore, subject to large irradiation-induced shrinkages.

2.3. Large HTGR reactors

The current fuel rod fabrication process for large HTGR commercial designs of 770 and 1160 MW (e) [55] has changed from that for the FSV demonstration plant only in the final carbonization step. To streamline production, green rods are now loaded directly into fuel blocks and carbonized in place (CIP), whereas FSV rods were carbonized in powdered beds and then inserted into fuel blocks. A two-stage, continuous-throughput furnace over 15 m long has been designed to accomplish the CIP step, and 45 fuel blocks containing some 70 000 fuel rods can be processed every 24 h. This fuel-rod throughput has been designed to match the output of green rods from the fully automated injection-moulding machine, which has 8 stations of 40 moulds each that turn full cycle in 6 min.

This completes the evolution of the present fabrication process for large HTGR fuel rods, which was briefly summarized in the beginning of Section 2. All discussion to this point has concerned work done by others, primarily at General Atomic Company (GAC) and at Oak Ridge National Laboratory (ORNL), that has not previously been reviewed to any extent, certainly not in the context of composite technology where it has a place. This review was considered necessary to set the stage for some original work to be reported in Section 3.

3. Research toward variant process for refabrication

All of the discussion to this point has concerned fresh-fuel fabrication, but it will eventually be necessary to refabricate fuel using fissile particles containing U-233 that has been recovered from fertile particles during spent fuel reprocessing [56]. This U-233 bred in thorium during reactor operation will contain traces of U-232, which emits highly penetrating gamma rays during its decay process, and therefore fuel refabrication must be conducted remotely in a heavily shielded facility [56]. The 15 m long CIP furnace designed for fresh-fuel fabrication would constitute a distinct disadvantage in hot-cell refabrication, and the powdered-bed procedure of carbonization is not well suited for remote handling. Therefore, there is additional incentive to develop a thermosetting matrix that will allow free-standing carbonization of refabricated fuel, and promising work toward such a process variant will now be discussed.

3.1. Re-examination of matrix shrinkage during carbonization

It is well known that increased graphite filler content in an organic binder decreases its shrinkage during carbonization, but axial injection through close-packed fuel particles limits filler to about 40 wt % in the wet matrix mix (2.2.1.2), and shrinkages of thermosetting matrices tried previously were too large to work well at this filler level. Therefore, another method had to be found to reduce matrix shrinkage, and the particle-to-matrix bonding in thermosetting rods had to be reduced. To study unrestrained shrinkage, various types of matrix rods without particle inclusions were moulded and given the same two-stage heat treatment used on fuel rods. Pyrolysis effects on the bulk density, volume shrinkage, and binder char yield of representative matrix types are summarized in Table II. All of these matrix types are thermosetting and were carbonized free-standing, except for the reference pitch-based matrix (F) used in fresh fuel, which was included as a control in judging the carbonization performance of the other matrices, and the fugitive polystyrene additive (G) used to create porosity in certain matrix formulations.

If two components are mixed in a moulded rod having no porosity, and if neither component influences the shrinkage of the other during carbonization, then the percentage of volume shrinkage of the composite should follow the rule of mixtures if such relative shrinkage is independent of sample size. That is

$$\Delta V_c = \nu_1 \Delta V_1 + \nu_2 \Delta V_2,$$

where ν_i is the volume fraction of the ith component present in the composite and ΔV_i is the percentage of volume shrinkage for a rod made from component i alone. For the cases in Table II, the graphite filler does not shrink ($\Delta V_2 = 0$) and the volume fraction of the binder is obtained from the weight fractions listed by

$$\nu_1 = \rho_2 \times \text{wt}\,\%\,(1)/[\rho_2 \times \text{wt}\,\%\,(1) + \rho_1 \times \text{wt}\,\%\,(2)].$$

The shrinkage behaviour of an unmodified thermosetting resin (A) at 1800° C will be examined first,

TABLE II Pyrolysis effects on carbon-yielding matrix compacts without particle inclusions

Cured matrix composition			Heat treatment temperature							
Binder		Filler†	200°C	900°C			1800°C			
Constituents	wt%	wt%	ρ(g cm^{-3})	ρ(g cm^{-3})	$-\Delta V$(%)	CY(%)	ρ(g cm^{-3})	$-\Delta V$(%)	CY(%)	% Char
Resinox (A)	100	0	1.27	1.39	45.6	59.6	1.42	48.6	57.8	100.0
	68	32	1.46	1.49	27.8	61.5	1.63	35.1	59.4	55.8
	50	50§	1.59	1.63	21.8	60.2	1.74	28.0	57.9	36.7
	30	70§	1.59	1.57	10.8	60.4	1.63	14.4	58.7	20.1
Varcum (B)	76	24	1.44	1.57	36.8	59.2	1.63	39.8	58.4	64.9
	60	40	1.57	1.65	26.7	61.6	1.72	30.6	60.0	47.4
Howmet (C)*	57	43	1.58	1.57	25.3	54.6	1.59	27.0	53.0	40.9
SC–1008 (D)*	48	52	1.56	1.54	25.2	45.7	1.64	30.7	44.1	28.9
91–LD (E)*	51	49	1.52	1.45	24.0	46.8	1.49	26.7	45.4	32.1
Pitch (F)	62	38	1.42	1.02	16.2	35.8	1.18	30.7	31.8	34.2
Polystyrene (G)	100	0	1.05	–	–	3.0	–	–	2.7	100.0
A–F	40–28	32	1.41	1.24	27.0	47.1	1.30	32.7	44.4	48.5
	28–22	50§	1.55	1.36	13.9	51.5	1.42	19.2	48.2	32.5
A–G	40–28	32	1.36	0.97	24.8	31.7	1.02	30.5	30.2	19.3
	28–22	50§	1.52	1.17	12.7	35.0	1.23	17.9	33.3	25.0
A–F–G	53–14–19	32	1.36	1.01	20.7	39.4	1.09	28.6	36.9	44.0
	30–13–17	40	1.44	1.08	18.6	35.5	1.18	26.9	33.4	33.4
	26–10–14	50§	1.52	1.24	14.0	39.9	1.27	17.6	37.6	27.3
	23–9–12	56§	1.53	1.25	9.9	35.6	1.28	13.2	33.3	20.7
B–F	36–25	39	1.49	1.46	27.1	53.1	1.53	31.0	51.9	44.8
C–G†	27–31	42	1.42	0.95	20.1	20.2	0.95	21.8	18.4	20.3
D–G†	21–34	45	1.45	0.90	9.2	20.8	0.94	15.2	18.2	18.2
E–G†	23–33	44	1.44	0.92	12.2	21.5	0.95	17.1	18.5	19.1
D–G	14–43	43	1.42	0.81	6.6	17.3	0.83	10.3	16.0	17.5

A. Resinox is a phenolic consisting of 11 parts of Monsanto's Resinox 754 to 9 parts of Resinox 755.
B. Varcum is a furan resin (Varcum 8251) that has been catalysed with 3%) OX260 from Quaker Oats Co.
C. Howmet is a proprietary binder supplied for evaluation by Howmet Corporation (Whitehall, Mich.); it consists of 87% solids dissolved in a volatile solvent.
D. Resinox SC–1008 is a Monsanto solvated phenolic containing 62% resin solids.
E. 91–LD is a solvated resin from U.S. Polymeric that contains 69% resin solids.
F. Pitch refers to General Atomic's reference thermoplastic binder; it is added to resins in small enough proportions that they remain thermosetting.
G. Polystyrene is a fugitive thermoplastic additive used to lower the char yield of thermosetting binders.
*The original matrix mixtures for these three solvated resins were all 60 wt% binder and 40% filler, but the compositions of the cured pieces differ because of the different amounts of solvents that are eliminated during cure.
†The three original matrix mixtures here had identical compositions of 30 wt% solvated resin, 30% polystyrene, and 40% filler.
‡The powdered graphite filler used throughout was Lonza KS-15, with 95% of the grains having sizes less than 15 μm.
§These filler contents in the binders in question are not injectable through 63.5 mm particle beds at pressures below 100 kg cm^{-2}; therefore, these matrix compositions are not candidates for fuel-rod injection, but were investigated only to gain information on the effects of filler content on matrix shrinkage during heat treatment.
All values listed are averages of measurements for at least three rods.

where $\rho_1 = 1.27\,\mathrm{g\,cm^{-3}}$, $\rho_2 = 2.20\,\mathrm{g\,cm^{-3}}$, and $\Delta V_1 = -48.6\%$. The measured shrinkages of Table II are compared to rule-of-mixture predictions in Fig. 5, and the agreement is reasonably good all the way out to 56 vol% filler (70 wt%), where the close-packed graphite powder begins to limit shrinkage. What this means is that for an injectable matrix mixture the filler does not significantly reduce the shrinkage percentage of the binder phase, it only reduces the volume fraction of binder present by virtue of the volume which it occupies. This being the case, a given volume percentage of porosity left in a fired matrix rod should have roughly the same effect on carbonization shrinkage as would the same volume percentage of filler in the green rod.

Therefore, a low-char-yield matrix additive such as polystyrene, which virtually disappears during heat treatment, should be very effective in reducing bulk shrinkage if some of the void space

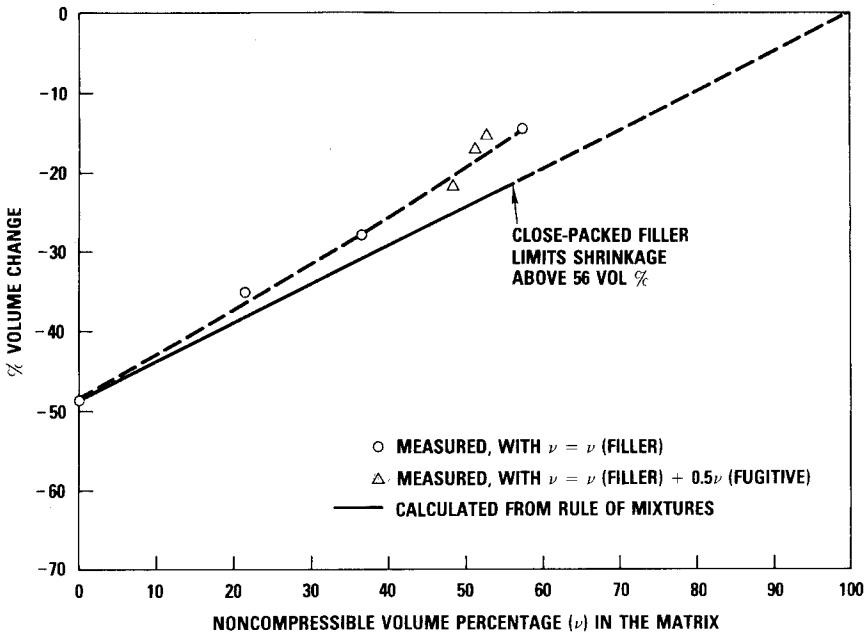

Figure 5 Matrix shrinkages at 1800° C compared to rule-of-mixture predictions.

that it leaves is maintained during carbonization. In other words, let us say that one isolates a small blob of polystyrene in a green matrix plug, follows its volatilization during heat treatment, and finds a pore left there in the matrix char. Then as far as gross shrinkage goes, this small void space might just as well have been occupied by a filler particle. It is clear from an examination of the data of Table II that something of this kind occurs. When half of the binder phase of uncured matrix formulations C through E was replaced with polystyrene (C–G through E–G), for example, the bulk volume shrinkage at 1800° C was reduced from between 20 to 60%.

Closer analysis reveals that a given volume fraction of polystyrene in a green thermosetting rod is roughly half as effective in reducing shrinkage at 1800° C as the same amount of filler, indicating that about half of the void volume left by the polystyrene remains unfilled following carbonization shrinkage. Thus in the examples above (C–G through E–G), if one calculates the percentage of volume dilution in the green rod that produces inaccessible volume in the fired rod as $\nu = \nu(\text{filler}) + 0.5\,\nu(\text{polystyrene})$, then the three resulting triangular points of Fig. 5 are in excellent agreement with shrinkage data for an undiluted thermosetting matrix. Hence, injectable thermosetting matrix mixtures have been obtained that have heat-treatment shrinkages comparable to undiluted resins with about 65 wt % graphite filler, which could not themselves be injected. Fig. 6 shows the structure of a thermosetting matrix (the same one shown in Fig. 1) in which half of the binder has been replaced with polystyrene. This matrix is seen to be much more space filling and internally porous than the undiluted matrix of Fig. 1; indeed, it looks very similar to the pitch-based matrix shown in Fig. 3. Moreover, the porosity introduced has weakened particle-to-matrix bonding in Fig. 6 to the point where slight separation is obtained at the interface during heat treatment. Therefore, the low-char additive solves both the shrinkage and strong bonding problems inherent to an undiluted thermoset.

In the light of the better understanding of carbonization behaviour that has been developed, let us now re-examine the matrix performances discussed in Section 2.2.2 by comparing the behaviours of an undiluted thermosetting matrix (A) and of the reference pitch-based matrix (F) used in fresh-fuel fabrication. The fundamentally different nature of their carbonization behaviours is well illustrated in Fig. 7, where the density data of Table II are plotted against heat-treatment temperature (HTT). Shrinkage is somewhat more rapid than weight loss in the undiluted resin, which densifies with HTT; the pitch matrix loses weight much more rapidly than volume, and consequently its density falls off very sharply. The primary

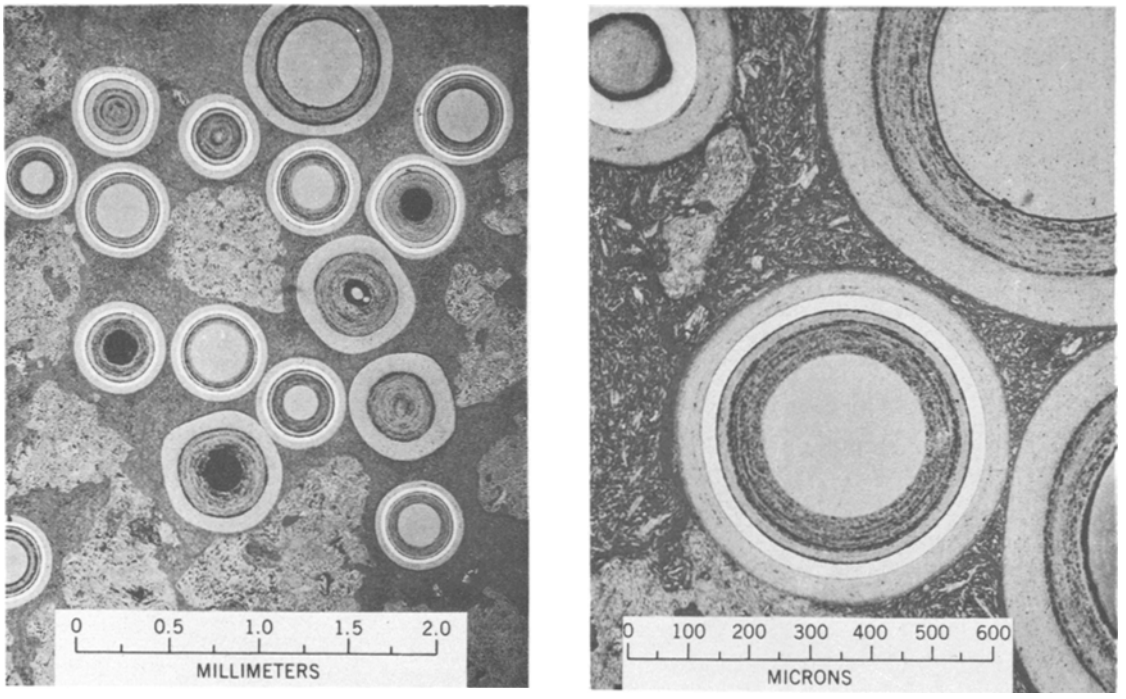

Figure 6 Matrix structure in a diluted thermosetting rod.

reason for this, of course, is that the thermoplastic pitch matrix leaves a porous char, whereas the undiluted thermosetting resin does not. As molecules within the highly cross-linked resin volatilize, the remaining interlinked chains of molecules react to largely close any internal pores through gross shrinkage of the matrix [57], whereas the pores that are formed in the uncrosslinked pitch matrix are left largely unfilled. Thus, gross shrinkage in thermosets is traded for internal porosity in thermoplastics, and the latter is needed in close-packed fuel rods because of bond strengths as well as shrinkages. It is now known, however, that such internal porosity can be introduced into a thermoset by the addition of a low-char-yield additive, such as polystyrene. Indeed, the density of such a diluted thermosetting matrix (C–G) falls off even more sharply than does that of pitch (Fig. 7).

3.2. Optimum dilution for a thermosetting matrix

The addition of a low-char additive to limit shrinkage and particle-to-matrix bonding in a thermosetting fuel rod seems to work best when the resin and fugitive are dissolved in a solvent to which graphite flour is added to form a matrix mixture that has the consistency of putty at room temperature. This mixture is then heated just prior to injection to reduce its viscosity. Cure of the resins used did not begin until the solvent had evaporated almost entirely, so that pot-life of the solvated resin was relatively long at temperatures below the boiling point of the solvent ($\sim 80^\circ$ C). Most injection work to date has been done at 150° C, with a dwell time of about a minute at that temperature before injection. Cure is effected in less than 5 min when the mould is held at 200° C. In addition to its value in mixing of binder components, the boiling solvent carries its share of graphite filler into the rod during injection and then evaporates during cure. This introduces some porosity into the green rod (from 2 to 5 vol %), which seems to be beneficial during carbonization, and increases the ratio of filler to binder char in the fired rod.

Shrinkage cracking of such diluted thermosetting rods during carbonization was observed to decrease steadily as the weight ratio of binder char to filler in the fired matrix decreased with the addition of more and more fugitive, but beyond a certain point the increasingly porous matrix became too weak for adequate bonding, and particles could be easily chipped from the outer rims of rods (especially from the weaker rim farthest from the injection end). Based on carbonization behaviour alone, with irradiation tests yet to follow, the

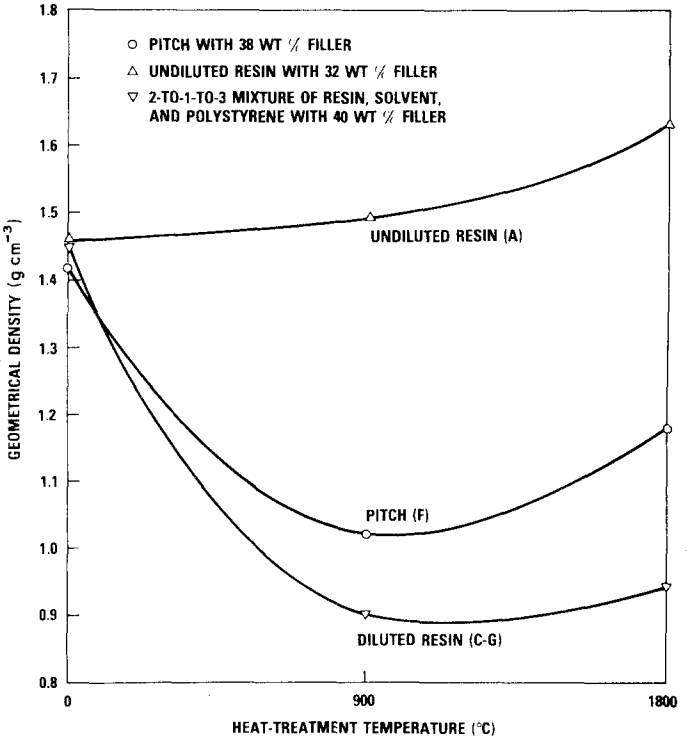

Figure 7 Density changes of various organic matrices with heat treatment.

optimum amount of binder char in the matrix of a fired rod was about 20 wt %. This corresponds to a wet matrix mixture consisting of roughly equal parts of resin and polystyrene dissolved in a quantity of solvent equal to 20% of their combined weight, with sufficient graphite filler being added (two thirds of the weight of the solvated binder above) to account for 40% of the weight of the total mix. Several commercial solvated resins of the type developed for impregnation of substrates in carbon–carbon composites work very well for this application when properly mixed with a fugitive and a filler, with Monsanto's SC-1008 (62 wt % resin solids) being perhaps the best of those tested. Lightly loaded fuel bodies made in Europe from admix compaction of graphite-filled thermosetting binders contain binder chars that constitute only about 10 to 12% of the fired matrix weight. However, the low ratio of binder char there is gained through increased filler content (80 wt %), which produces a dense matrix with good strength, rather than through low-char additives that are necessary for injected rods with only 40 wt % filler.

3.3. Irradiation testing of a diluted thermosetting matrix

To complete the assessment of a diluted thermosetting matrix for use in refabricated fuel rods, irradiation screening tests of such rods are being conducted in three capsule experiments: HB-2, HRB-11, and HRB-12. The shorter HB-2 test was designed to receive a fast-neutron fluence of 5×10^{21} n cm^{-2} ($E > 0.18$ MeV) at a temperature of 1200° C, and it has recently been completed. The other two capsules are to be irradiated to the full HTGR design fluence of 8×10^{21} n cm^{-2} at 1350° C, and results of these experiments will not be available until early in 1977. Thirty three fuel rods were included in these tests, 17 in HB-2 and 8 in each of the others. A reference pitch-based rod was included in each capsule to serve as a control for judging the irradiation performances of the 30 thermosetting rods. Binder types and low-char additives were varied to give fired rods in which the binder char contributed from 12 to 48% of the matrix weight [58], bracketing the optimum 20% value for carbonization performance, where the graphite filler content of all rods accounted for about 40 wt % of the uncured matrix mixture.

Initial results from the HB-2 irradiation are very encouraging in that diluted thermosetting rods seem to perform about as well as the reference pitch-based rod [59]. The representative appearance of such rods before and after irradiation is illustrated in Fig. 8, and the matrix structure within this same rod is shown in Fig. 9. Particles are more visible on the surface of the rod and

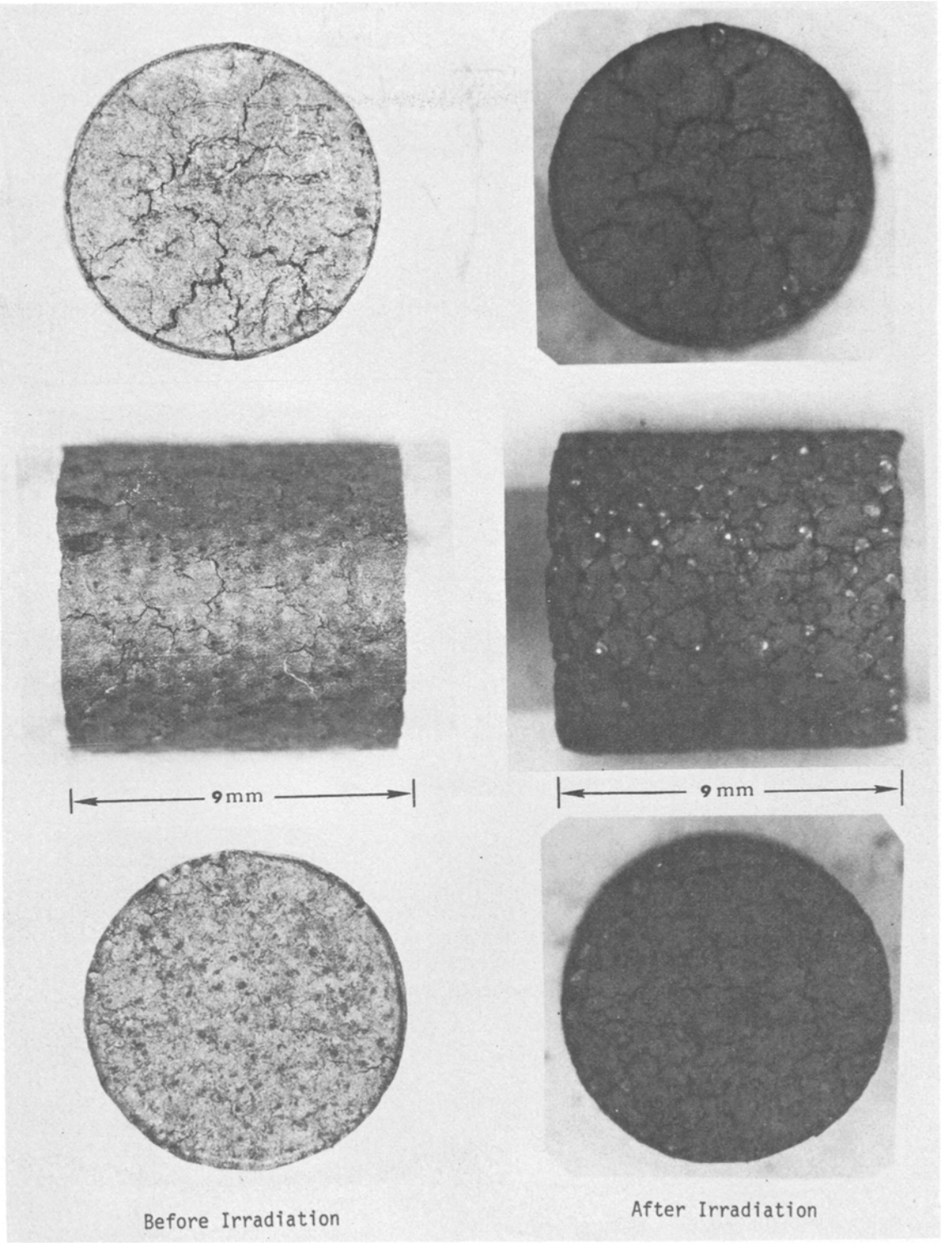

Figure 8 Appearance of a typical diluted thermosetting rod before and after irradiation (5×10^{21} n cm^{-2} at 1200° C).

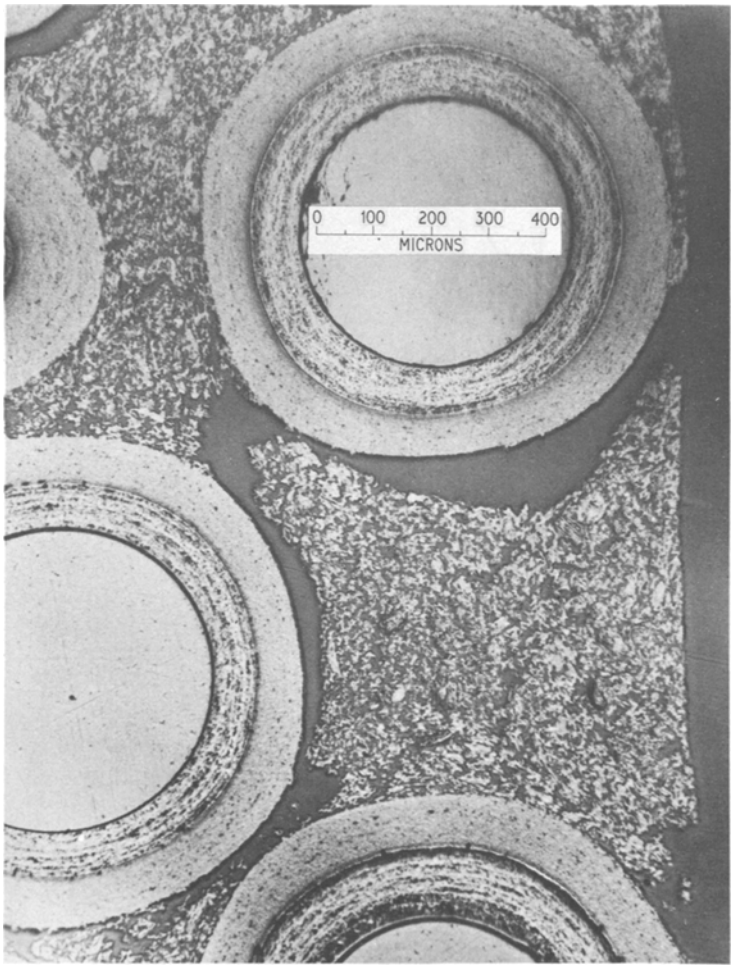

Figure 9 Post-irradiation matrix structure and nature of surface cracking in a diluted thermosetting rod.

cracking has worsened, indicating that the matrix has undergone additional irradiation-induced shrinkage, but particle retention of the rod is still adequate. Actually, the rod integrity is better than it appears to be, since many of the surface cracks extend only one particle diameter in depth (Fig. 9). Moreover, pyrocarbon coatings on fuel particles have not been damaged by excessive particle-to-matrix bonding during irradiation to a fluence of 5×10^{21} n cm^{-2}, and because of the nature of the interface no coating damage is anticipated in the full-fluence irradiations (8×10^{21} n cm^{-2}) that are still underway.

A definitive test for coating damage in an irradiated rod is provided by subjecting the rod to a short neutron exposure of known intensity in GAC's TRIGA reactor, and then collecting and counting the radioactive Kr-85m fission gas that is released from the rod during heat treatment to 1100° C. The ratio of the number of such short-lived atoms released (R) to the total number born (B) during the TRIGA exposure gives an accurate measure of coating damage, since atoms will be released from kernels only if coatings are compromised. Nine thermosetting rods with less than 32 wt % binder char in their matrices were individually tested in this way, and all had R/B values in the 10^{-6} to 10^{-5} range [59], indicating negligible coating damage. Likewise, R/B for the reference pitch-based matrix with 36 wt % binder char was in this same range. However, R/B values for lightly diluted thermosetting rods with binder chars ranging from 34 to 48 wt % were greater than 10^{-4}, indicating that particle-to-matrix bonding was sufficiently strong here to damage coatings.

It is noteworthy that the coating damage that first begins to occur as the percentage of binder char increases is restricted almost exclusively to fissile particles, which have thinner outer layers of PyC that may not be too well bonded to the

underlying SiC layer. The fertile particles did not begin to be damaged to any extent until the binder char in the matrix exceeded 44 wt %. The photomicrographs of Fig. 2 were for a rod with no fugitive (48 wt % binder char) in which both types of particles were damaged. Post-irradiation matrix structures for thermosetting formulations with the preferred 20 wt % binder char and the coating-damaging 44 and 48 wt % chars are compared to that of the reference pitch rod in Fig. 10, and the density differences are quite clear. Fortunately, the types of thermosetting rods that performed best during screening for carbonization behaviour are also the ones that did best on irradiation in HB-2, and rods of these types were selected almost exclusively for the HRB-11 and -12 irradiations that are in progress. These latter experiments will provide a critical test of the mechanical integrity of highly diluted thermosetting rods under full-fluence irradiation*. The HB-2 test was unduly severe in this regard for the fluence in question, however, since carbonization cracking was initially worse for these small rods (9.2 mm diameter) than for the larger rods (12.4 mm diameter) still under irradiation [58]. Therefore, the performance of these better as-made rods is expected to be satisfactory for full-fluence irradiation.

4. Conclusions with possible applications to other carbon–carbon technologies

Injection-moulded fuel rods for the HTGR must be fabricated in such a way that the carbonaceous matrix and/or its interface with pyrocarbon-coated fuel particles always gives way under carbonization and irradiation shrinkages before pressure-vessel coatings on fuel particles are damaged. This places fuel rods at the opposite extreme from structural carbon–carbon composites, where the desire in ultimate testing is always to have the stronger fibrous reinforcements fail before the weaker matrix does in order to realize the full load-carrying potential of the structure during service. The other requirement of the organic binder in close-packed fuel rods is that shrinkages during carbonization and subsequent irradiation should be as small as possible in order to limit matrix damage to the extent that particle retention is not jeopardized.

This dual requirement of weak particle-to-matrix bonding and limited shrinkage is better satisfied by a thermoplastic pitch-based matrix than by an unmodified thermosetting matrix. This has also been found to be the case in the carbonization of fibrous-reinforced composites [48–50], where the combination of high shrinkage and strong bonding of thermosetting binders often crack composites and damage fibres. Consequently, a pitch-based matrix was selected as the standard for fresh-fuel fabrication, and such fuel rods have demonstrated excellent performance in many full-fluence irradiation tests [60]. These thermoplastic fuel rods must be constrained during carbonization in order to maintain their shape however, and the free-standing carbonization afforded by thermosetting rods would be of advantage in remote fabrication of reprocessed spent fuel if the problems of shrinkage and strong bonding can be controlled. There are at least two ways to reduce carbonization shrinkage of any organic binder: (1) add the maximum amount of nonshrinking filler that can be injected within pressure limitations imposed by the coated particles (40 wt % powdered graphite), as had been done previously, and (2) replace part of the binder with a low-char-yield additive (fugitive) that produces a porous char. This second unexplored method not only reduces shrinkage markedly for thermosetting matrices, because of the introduction of internal porosity of the type that is found naturally in char from pitch [48], but it also reduces particle-to-matrix bonding to acceptable levels.

The optimum class of diluted thermosetting matrix of this type for injection of fuel rods consisted of roughly equal parts of resin and fugitive (polystyrene) dissolved in a quantity of solvent equal to 20% of their combined weight, with graphite flour equal to two-thirds of the weight of this solvated mixture being added to bring the filler content in the final mixture up to 40 wt %. A matrix that performed very well was obtained by dissolving 6 parts of powdered polystyrene in 9 parts of Monsanto's commercial solvated phenolic SC-1008, which is widely used in the initial impregnation of structural carbon–carbon composites [51, 52], and then mixing in 10 parts of graphite flour. Injectable diluted mixtures of this type with 40 wt % filler undergo unrestrained shrinkages on carbonization that are as small as those of undiluted resins with 65 wt % filler, which would not be injectable axially. Moreover, the

*These full-fluence rods have recently been discharged from the reactor, and mechanical integrities were satisfactory for all rods in which the binder char in the matrix constituted at least 17 wt %.

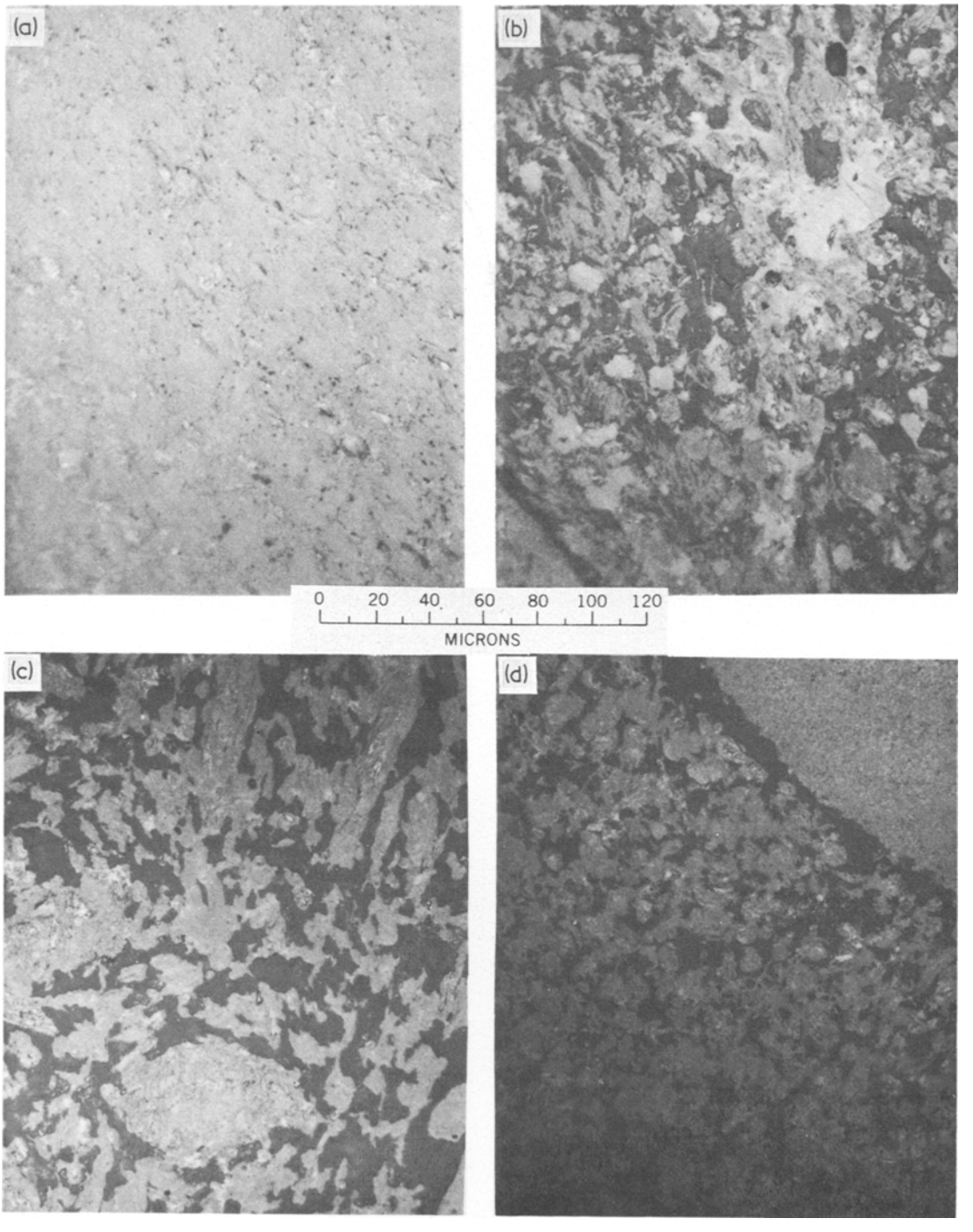

Figure 10 Matrix structures for thermosets with: (a) no dilution (48 wt % char), (b) light dilution (44 wt % char), and (c) near-optimum dilution (20 wt % char) compared to that for (d) a thermoplastic pitch-based matrix.

porous fired matrix that results contains only about 20 wt % binder char, which is the less stable component under irradiation. Because of the limited shrinkage of the diluted thermosetting matrix during both carbonization and irradiation, fuel rods are less prone to distortion and hairline surface cracking than are rods fabricated from undiluted thermosets, with appearances of such fired rods before and after irradiation being comparable to those of pitch-based rods. More importantly,

because of this limited shrinkage in conjunction with weak particle-to-matrix bonding, there is no damage to coatings on fuel particles during carbonization or irradiation. Particle damage only began to occur during irradiation for those lightly diluted thermosetting rods in which the fugitive in the uncured matrix had been reduced to the point where the less stable binder char accounted for more than 32 wt% of the fired matrix [59].

When structural carbon–carbon composites are made from the initial pyrolysis of fibrous-reinforced organic binders followed by multiple reimpregnation and heat treatment to develop strength, it appears that the primary function of the initial binder is to leave a porous matrix amenable to impregnation that: (1) does not damage fibres through excessive bonding and subsequent shrinkage, and (2) provides a sound skeletal structure free of distortion or gross cracking. A thermoplastic pitch binder has been shown to perform this function better than undiluted thermosetting resins, but such resins have continued to be used for the most part, perhaps because of the easier processing provided by unrestrained carbonization. It is suggested that the diluted thermosetting matrix developed for fuel rods might give even better initial carbonization performance than pitch, while retaining the desired processing advantages. Thus, while the desired end products are quite different, techniques developed for the fabrication of fuel rods might be of some benefit in the initial carbonization step for structural composites and vice versa, since goals here are somewhat similar.

Acknowledgements

The author wishes to acknowledge the investigators at GAC, ORNL, and elsewhere who developed the fabrication process for fresh fuel that is described. He is also indebted to Drs. R. Dahlberg, W. Goeddel, and J. Watson for envisioning and encouraging the work on the thermosetting matrix. Appreciation is also expressed to Mr. T. Tagami for experimental assistance and to Drs. J. Sheehan, C. Young, S. Sterling, and J. Kaae for a variety of valuable suggestions and contributions.

References

1. R. E. WALKER and T. A. JOHNSTON, *Nucl. Engr. Intl.* **14** (1969) 1069.
2. R. C. DAHLBERG, R. F. TURNER and W. V. GOEDDEL, *ibid* **14** (1969) 1073.
3. H. B. STEWART, R. C. DAHLBERG, W. V. GOEDDEL, D. B. TRAUGER, P. R. KASTEN and A. L. LOTTS, in "Proceedings of the 4th International Conference on the Peaceful Uses of Atomic Energy", Vol. 4 (United Nations, Geneva, 1971) p. 433.
4. V. S. BOYER, J. P. GIBBONS, T. A. JOHNSTON, R. J. HOE, D. K. FELDTMOSE and W. C. DROTLEFF, *Nucl. Engr. Intl.* **19** (1974) 635.
5. R. C. DAHLBERG and L. H. BROOKS, *ibid* **19** (1974) 640.
6. W. V. GOEDDEL and J. N. SILTANEN, in "Annual Review of Nuclear Science", Vol. 17, edited by E. Segrè, G. Friedlander and H. P. Noyes (Annual Reviews Inc., Palo Alto, California, 1967) p. 189.
7. J. C. BOKROS, in "Chemistry and Physics of Carbon", Vol. 5, edited by P. L. Walker Jr. (Marcel Dekker, New York, 1969) p. 1.
8. L. R. SHEPHERD, *J. Brit. Nucl. Energy Soc.* **9** (1970) 173.
9. K. S. B. ROSE, *J. Inst. Nucl. Eng.* **12** (1971) 95.
10. H. HICK, *Nucl. Eng. Des.* **28** (1974) 367.
11. N. PICCININI, in "Advances in Nuclear Science and Technology", Vol. 8, edited by E. J. Henley and J. Lewins (Academic Press, New York, 1975) p. 255.
12. R. B. DUFFIELD, *J. Brit. Nucl. Energy Soc.* **5** (1966) 305.
13. W. V. GOEDDEL, *Nucl. Appl.* **3** (1967) 599.
14. M. S. T. PRICE, J. R. G. GOUGH and G. W. HORSLEY, *J. Brit. Nucl. Energy Soc.* **5** (1966) 361.
15. R. A. U. HUDDLE, in "Advanced and High Temperature Gas-Cooled Reactors" (IAEA, Vienna, 1969) p. 631.
16. M. S. T. PRICE and L. R. SHEPHERD, International Conference on Physical Metallurgy of Reactor Fuel Elements (Gloucestershire, England, 2–7 September 1973); USAEC Report CONF-730912.
17. M. R. EVERETT, F. RIDEALGH and E. H. VOICE, Dragon Project Fuel Performance Meeting (London, 4–5 December 1973) paper 10; D.P. Report 876.
18. M. R. EVERETT and R. BLACKSTONE, BNES International Conference on Nuclear Fuel Performance (London, 15–19 October 1973) paper 29; USAEC Report CONF-731004.
19. L. W. GRAHAM, M. S. T. PRICE, R. A. SAUNDERS and E. SMITH, ANS Topical Meeting on Gas-Cooled Reactors (Gatlinburg, Tennessee, 7–10 May 1974) USAEC Report CONF-740501.
20. L. AUMÜLLER, K. H. HACKSTEIN, M. HROVAT, E. BALTHESEN, B. LIEBMANN, K. EHLERS and K. RÖLLIG, in "Proceedings of the 4th International Conference on the Peaceful Uses of Atomic Energy", Vol. 4 (United Nationa, Geneva, 1971) p. 415.
21. E. BALTHESEN and H. RAGOSS, International Conference on Physical Metallurgy of Reactor Fuel Elements (Gloucestershire, England, 2–7 September 1973); USAEC Report CONF-730912.
22. G. IVENS, M. WIMMERS and H. RAGOSS, BNES International Conference on Nuclear Fuel Performance (London, 15–19 October 1973) paper 43; USAEC Report CONF 731004.

23. E. BALTHESEN, K. EHLERS, K. G. HACKSTEIN and H. NICKEL, ANS Topical Meeting on Gas-Cooled Reactors (Gatlinburg, Tennessee, 7–10 May 1974) USAEC Report CONF-74051.
24. J. RAYMOND, CERCA Report 339 (February 1975).
25. *Idem,* CERCA Report 345 (August 1975).
26. D. F. ADAMS and S. W. TSIA, *J. Composite Mater.* **3** (1969) 368.
27. R. K. McGEARY, *J. Am. Ceram. Soc.* **44** (1961) 513.
28. K. GOTOH and J. L. FINNEY, *Nature* **252** (1974) 202.
29. J. D. BERNAL and J. MASON, *ibid* **188** (1960) 910.
30. G. B. SCOTT, *ibid* **194** (1962) 956.
31. J. D. BERNAL, *ibid* **183** (1959) 141.
32. *Idem, Proc. Roy. Soc. Lond.* **A280** (1964) 299.
33. G. D. SCOTT, A. M. CHARLESWORTH and M. K. MAK, *J. Chem. Phys.* **40** (1964) 611.
34. S. YERAZUNIS, S. W. CORNELL and B. WINTNER, *Nature* **207** (1965) 835.
35. S. YERAZUNIS, J. W. BARTLETT and A. H. NISSAN, *ibid* **195** (1962) 33.
36. D. R. HUDSON, *J. Appl. Phys.* **20** (1949) 154.
37. J. M. ROBBINS, R. L. HAMNER and H. BEUTLER, in Oak Ridge National Laboratory Report ORNL-4429 (August 1969) p. 83.
38. J. L. SCOTT, J. A. CONLIN, J. H. COOBS, D. M. HEWETTE, J. M. ROBBINS, R. L. SENN and B. H. MONTGOMERY, Oak Ridge National Laboratory Report ORNL-TM-3640 (March 1972).
39. USAEC Report GA-9720 (October 1969) p. 56.
40. J. H. COOBS, J. L. SCOTT, B. H. MONTGOMERY, J. M. ROBBINS, C. B. POLLOCK and J. A. CONLIN, Oak Ridge National Laboratory Report ORNL-TM-3988 (January 1973).
41. USAEC Report Gulf-GA-A10980 (January 1972) p. 37.
42. G. R. TULLY, A. S. SCHWARTZ and W. V. GOEDDEL, *Carbon* **4** (1966) 51.
43. M. T. SIMNAD, Gulf General Atomic, (unpublished data).
44. I. M. DANIEL and A. J. DURELLI, *Expt. Mech.* **2** (1962) 240.
45. A. J. DURELLI and V. J. PARKS, *ibid* **3** (1963) 263.
46. T. KOUFOPOULOS and P. S. THEOCARIS, *J. Composite Mater.* **3** (1969) 308.
47. H. A. MACKAY, *Carbon* **8** (1970) 517.
48. E. FITZER and B. TERWIESCH, *ibid* **10** (1972) 383.
49. E. FITZER and B. TERWIESCH, 10th Biennial Conference on Carbon (Bethlehem, Pennsylvania, 27 June–2 July 1971) p. 62.
50. E. FITZER, M. HEYM and K. KARLISCH, 4th International Carbon and Graphite Conference (London, 23–27 September 1974) paper 106.
51. J. L. PERRY and D. F. ADAMS, *J. Mater. Sci.* **9** (1974) 1764.
52. *Idem, Carbon* **14** (1976) 61.
53. W. V. KOTLENSKY, in "Chemistry and Physics of Carbon", Vol. 9, edited by P. L. Walker Jr and P. A. Thrower (Marcel Dekker, New York, 1973) p. 173.
54. B. GRANOFF, H. O. PIERSON and D. M. SCHUSTER, *Carbon* **11** (1973) 177.
55. J. W. LANDIS, *J. Brit. Nucl. Energy Soc.* **12** (1973) 367.
56. E. MERZ, *Kerntechnik* **15** (1973) 249.
57. E. FITZER and W. SCHÄFER, *Carbon* **8** (1970) 353.
58. R. E. BULLOCK, General Atomic Report GA-A13851 (April 1976).
59. R. E. BULLOCK and S. A. STERLING, General Atomic Report GA-A14229 (December 1976).
60. D. P. HARMON and C. B. SCOTT, General Atomic Report GA-A13173 (October 1975).

Received 2 November and accepted 17 November 1976.